RESEARCH ARTICLE

Macromolecular Materials and Engineering
Open Access
www.mame-journal.de

Reusable and Transparent Impaction-Based Filter with Micro Apertured Multiscale Polymeric Stencil for Particulate Matter Capture

Minju Kim, Gahyun Lee, Segeun Jang, Dong In Yu, and Sang Moon Kim**

Air pollution by particulate matter (PM) in the air including PM1.0, PM2.5, and PM10, which are categorized by particle size, is a critical global environmental issue, harming the climate, ecosystems, and human health. Especially, ultrafine dust including PM1.0 and PM2.5 poses significant human health risks. Commercial fabric-based filters effectively trap PMs but cause high-pressure drop and limited filter capacity and reusability. Electrospun nanofiber filters address some issues but have low mechanical strength, toxic exposure risks, long fabrication times, and restrained reusability. Herein, a reusable and transparent impaction-based PM filter using a UV-curable polymeric stencil with micro apertures is proposed. The polymeric stencil filters achieve high filter efficiency (68–94%), superior filter capacity, and low-pressure drop (<64 Pa). The polymeric stencil filters can be easily cleaned with water or ethanol and remain stable under extreme temperatures (−196 to 450 °C) with slight shrinkage (0–7%). The polymeric stencil filters can be broadly utilized for not only industrial, indoor, and vehicle filters but also transparent and flexible facial health masks.

1. Introduction

Severe air pollution originating from mobile vehicles, power generation plants, artificial detergent solvents, and wildfire smoke is one of the most serious global environmental issues. Particulate matter (PM) floating in the air influences climate change and threatens ecosystem and human health.[1–5] The PM, which is composed of complex compounds including ammonium, sulfate, nitrate, and carbon materials is categorized into PM1.0, PM2.5, and PM10 depending on the particle size.[6–8] And the latter number indicates the maximum aerodynamic diameter of the particles in the classification. When PMs are inhaled, they penetrate the human lungs and can cause serious respiratory and cardiovascular diseases. Especially, PM2.5 and PM1.0 can contribute to deadly diseases such as lung cancer, dementia, and heart attacks.[9,10] In this aspect, although reduction and suppression of the PM generation at the pollutant-generating source are important, the development of high-performance and high-capacity filters is very critical to reducing considerable risk to human health. In addition, after mankind has experienced a pandemic due to the virus, the significance of developing a mask filter that can capture ultrafine viruses and bacteria also becomes growing.[11] To address the issue, diverse kinds of conventional filters have been invented and manufactured. The commercially available filters including high-efficient particulate air (HEPA) filters and melt-blown nonwoven fabric filters are mostly composed of randomly stacked fibers. The densely packed thick layers of the filters can trap PM efficiently. Whereas the dense, thick, and tortuous layers with randomly stacked fibers induce non-recyclability and high-pressure drop, which needs more external energy for the filtering process.[12–14] To maintain high filtration efficiency while reducing pressure drop, extensive research has been conducted by focusing on reducing fiber diameter to the nanometer scale using the electrospinning process.[15–18] This process involves applying a high-voltage power supply to generate an electric field, which electrifies a liquid polymer solution droplet to produce a jet. Subsequently, the jet undergoes stretching and elongation, resulting in the production of stacked nanofibers with a diameter smaller than 200 nm.[19,20] With stacked nanometer-sized fibers, the surface area and porosity of the ultrathin filter are increased, and it leads to high filtration efficiency and relatively low-pressure drop compared to the commercial ones. And as the pore size gets decreased with the nanofibers, particle sieving from the nano-sized nets contributes to high

M. Kim, G. Lee, S. M. Kim
Department of Mechanical Engineering
Incheon National University
Incheon 22012, Republic of Korea
E-mail: ksm7852@inu.ac.kr
S. Jang
School of Mechanical Engineering
Kookmin University
Seoul 02707, Republic of Korea
D. I. Yu
Department of Mechanical Design Engineering
Pukyong National University
Busan 48513, Republic of Korea
E-mail: diyu@pknu.ac.kr
The ORCID identification number(s) for the author(s) of this article can be found under https://doi.org/10.1002/mame.202300285

DOI: 10.1002/mame.202300285

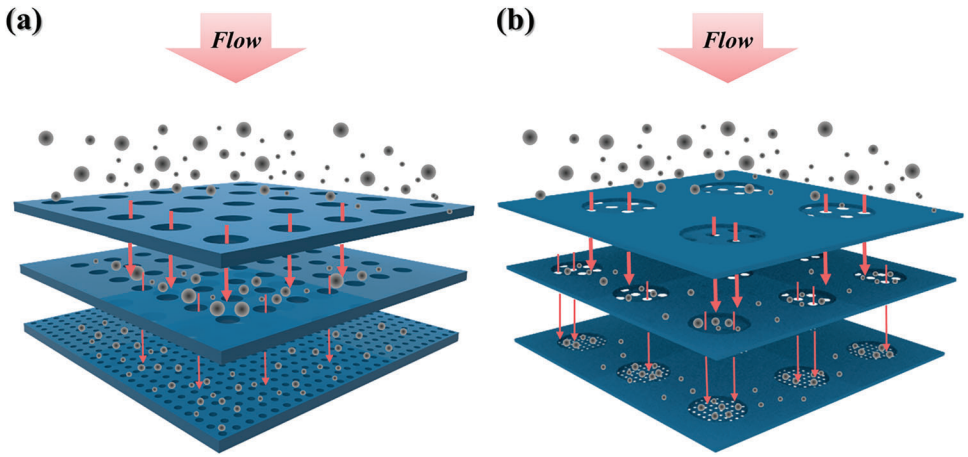

Figure 1. Schematic illustration of the impaction-based filter with micro apertured multiscale polymeric stencil. a) Stacked single-scale polymeric stencils, b) Stacked multi-scale polymeric stencils.

filtration efficiency in addition to the well-known filtration mechanism. Although the nanofiber-based filters exhibit high filtration efficiency and relatively low-pressure drop,[21] there are still remaining issues. Since the nanofiber-based filter is not freestanding, assembling on mesh-type mechanical support with sufficient adhesion force is required to be used as a filter. And as the fiber diameter decreases, the lowered mechanical strength of the filter limits the operating condition for the filtering. External physical load during handling and high flow-induced viscous force may destruct and collapse the nanofiber structures.[22] To improve the mechanical property of the filters, the stacked layer should be thicker. As the thickness of the filter increases, the filtration efficiency would be improved but the densely packed layers induce high-pressure drop. Furthermore, toxic and harmful solvents evaporate during the fabrication process, and high voltage over kV causes danger to workers. And long fabrication time and serial process make it challenging to fabricate large-area filters and commercialization. And as the commercial fiber filter cannot be reused due to the captured PM deep inside fibers, removal of the captured PMs is challenging. If the liquid solution is used for cleaning, the capillary-induced clustering during the evaporation would induce aggregation and collapse of the fibers.[23]

In this paper, we propose an impaction-based filter for capturing PM by using a porous and UV-curable polymeric stencil with a freestanding micro aperture array. To achieve optimal filter performance, single-scale, and multi-scale polymeric stencils were fabricated and applied as filters shown in **Figure 1**. The optimal performance with the impaction-based filters was investigated by varying the inlet face-velocity of particles, the spacing between polymeric stencils, and the stacking configuration. The porous polymeric stencil filter developed in this study has high filter efficiency of up to 58% (at PM1.0), 85% (at PM2.5), and 94% (at PM5.0) in the optimized configuration condition. And also, it showed a low-pressure drop in the range of 4–64 Pa, high filter capacity, and quality factor (QF) similar to commercial filters as 0.03. Compared to a previous study with an isoporous membrane filter, it can be verified that the developed and optimized polymeric filter is capable of maximizing the effect of the impaction mechanism, securing superior filter capacity, reducing pressure drop, and optimizing the filter performance by varying the operating conditions and configuration. As a result, sufficient filtration efficiency was achieved even at PM1.0, which is ultra-fine dust. In addition, the proposed polymeric filter can be reused by simply washing with water and shows excellent stability while maintaining its structure even when exposed to high temperatures at 450 °C and extremely low temperatures at −200 °C. The fabricated filter not only reduces environmental pollution through continuous reuse but also manufactures filters for industrial, indoor, and vehicle applications by easily controlling the size of stencils. Moreover, the flexibility and transparency, which are unique characteristics of the polymeric stencil can be applied to transparent facial health masks.

2. Results and Discussion

2.1. Filtration Performance of PUA Polymeric Stencils

It is essential to form straight apertures without clogging to effectively utilize the polymeric stencil as a filter with low flow resistance. To fabricate the stable-upright apertures in a polymer stencil, it is crucial to select a polydimethylsiloxane (PDMS) mold with a proper aspect ratio that can prevent structural deformation such as buckling phenomenon during the fabrication process. Based on the previous research, as a result of the investigation on the critical buckling load shown in Figure S1, Supporting Information, a PDMS mold with an aspect ratio (AR) below 1.3 was selected to prevent buckling. The specifications of the prepared PDMS mold are listed in Table S1, Supporting Information.[24] **Figure 2** and Figure S2, Supporting Information, show the OM images and cross-sectional scanning electron microscopy (SEM) images, respectively, of the polymer stencils used in the filter performance test. Two types of polymer stencils were prepared for the filter application: single-scale stencils with identical hole arrays (Figure 2a–c) and multi-scale stencils with overlapped holes of different sizes (Figure 2d–f). All the samples have a spacing ratio, which is defined as the space between holes divided by the aperture diameter as one. The single-scale stencils have pore

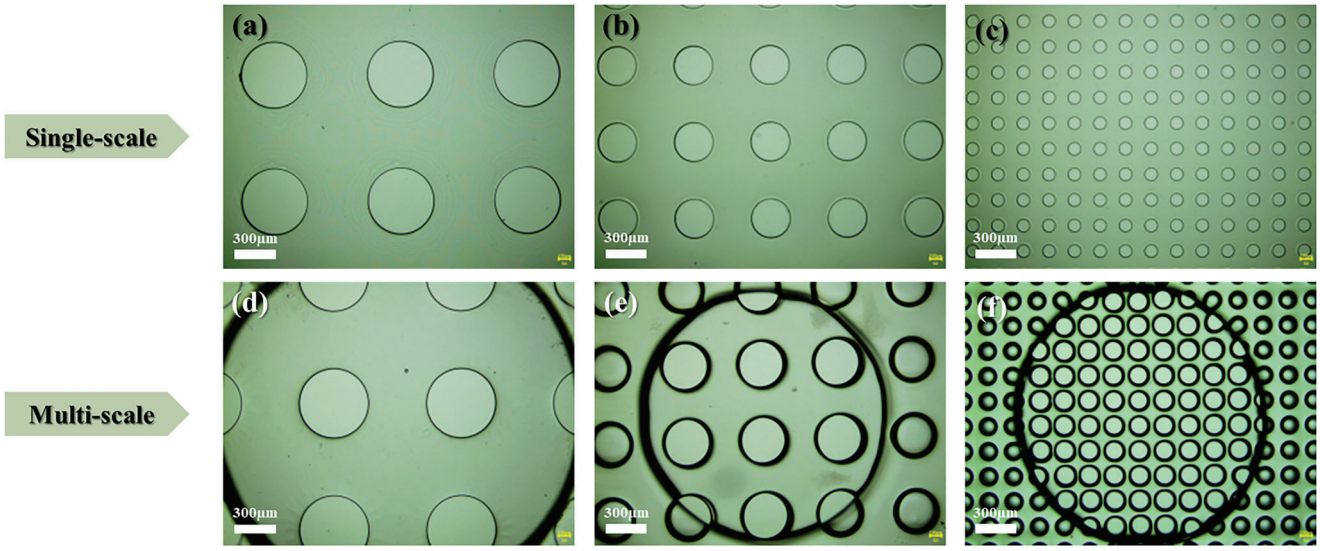

Figure 2. The OM images of polymer stencil used for the filter performance test. a–c) Single-scale stencil: a) 500 μm aperture, b) 300 μm aperture, and c) 100 μm aperture. d–f) Multi-scale stencil: d) 3000/500 μm aperture, e) 2000/300 μm aperture, and f) 2000/100 μm aperture.

sizes of 500, 300, and 100 μm, with thicknesses of 20, 120, and 120 μm, respectively. The multi-scale stencils have pore sizes of 3000/500, 2000/300, and 2000/100 μm, with thicknesses of 400, 320, and 320 μm for the respective samples. It is confirmed that the micro apertures of the polymer stencils remain stable and upright without buckling and bending for the filter performance test.

With the prepared polymer stencils, the filtering performance was measured by varying face velocity, spacing between stencils, and stacking configuration. The spacing between the polymeric stencil was controlled using a commercially available thin silicon rubber film to secure great air tightness. In Figure S3, Supporting Information, the filter performances with a variation of three factors of the stacked single-scale stencils with 500, 300, and 100μm-apertures were relatively compared. In the graphs, the *x*-axis represents the operating time, and the *y*-axis represents the amounts of outlet particles after passing through the polymeric stencil filters. The lower value of the measured amount of particles indicates the higher filter efficiency. Based on the results, the proper operating conditions are determined as follows:

- The inlet face velocity is 10 cm s−1 (Figure S3a, Supporting Information).
- The spacing between stacked polymeric stencils is 0.2 mm between stencils with 500 and 300 μm-apertures/0.1 mm between stencils with 300 and 100 μm-apertures (Figure S3b, Supporting Information).
- The polymeric stencils are assembled in a configuration where the diameter of the stencil apertures decreased toward the lower layer (Figure S3c, Supporting Information).

Similarly, in **Figure 3**a, the stacked multi-scale stencil filter showed the highest filtering efficiency when a particle inlet face velocity is 10 cm s^{-1}. Furthermore, when it comes to the spacing

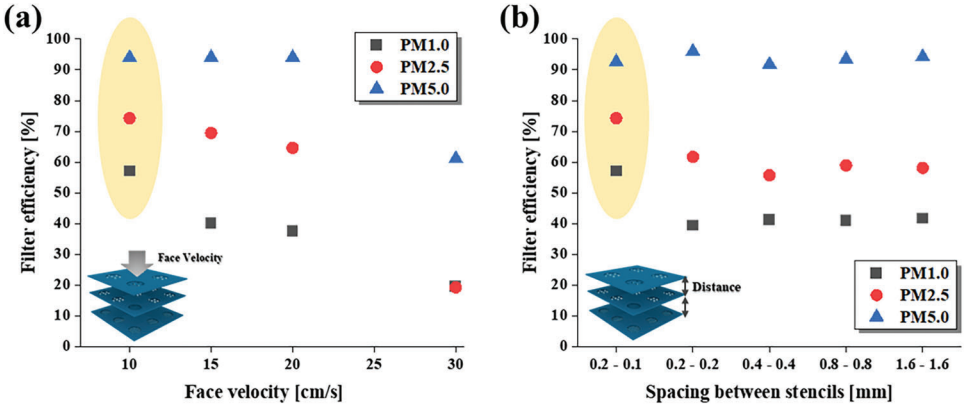

Figure 3. A plot of the filter efficiency with a variation of face velocity and spacing between stencils. a) Measured and calculated filter efficiency for the three different PM sizes depending on face velocity. b) Measured and calculated filter efficiency for the three different PM sizes depending on the spacing between stencils.

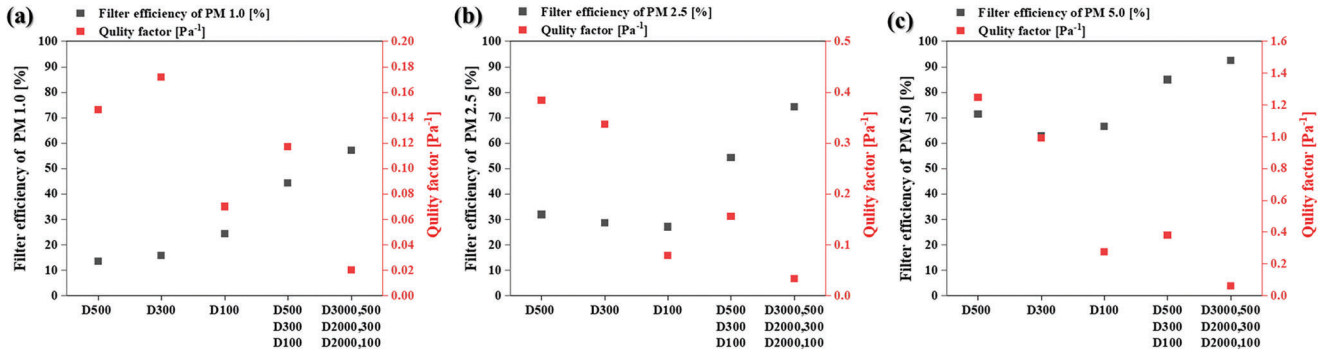

Figure 4. a–c) A plot of filter efficiency and quality factor (QF) of PUA stencil filters depending on the configuration of the stencils for PM1.0 (a), for PM2.5 (b), and for PM5.0 (c).

between stacked multi-scale polymeric stencils, it is necessary to gradually reduce the spacing toward the lower layer with smaller aperture sizes as shown in Figure 3b.

To evaluate the filter performance, the fabricated polyurethane acrylate (PUA) stencil filters were inserted into the experimental filtering setup and tested under the aforementioned operating conditions. Specifically, two configurations of PUA stencil filters were prepared: 1) a mono-layer filter with aperture diameters of D500, D300, and D100 μm, respectively, and 2) a three-stacked layer filter with single-scale stencils in a D500–D300–D100 μm configuration, as well as multi-scale stencils in a D3000/500–D2000/300–D2000/100 μm configuration. **Figure 4** shows the results of the filter efficiency and quality factor (QF) depending on the stencil filter configuration. The filter efficiency is calculated using Equation (1).[2,25]

$$\text{Filter efficiency, } \eta = \frac{\text{Amount of Inlet particles} - \text{Amount of Outlet particles}}{\text{Amount of Inlet particles}} \times 100\,[\%] \quad (1)$$

And the quality factor (QF) is a commonly used indicator for comparing the relative performance of filters. It is defined as $-\ln(1-\eta)/\Delta P$, where η represents filter efficiency and ΔP represents the pressure drop across the filter.[2,26] The pressure drop (ΔP) is the resistance to airflow passing through the filter, measured in pascals (Pa). **Table 1** shows the pressure drop values for the tested filters. Based on these factors, the results of PM1.0 filtering with mono-layer with a single-scale stencil exhibited extremely low-pressure drops, but significantly low filter efficiency in the range of 14–24% (Figure 4a). This suggests that the polymeric stencil filter with such configurations may not be suitable for use as a filter. However, a three-stacked layer configuration with single-scale stencils, which is D500–D300–D100 μm, resulted in an improved filter efficiency of 45%. A three-stacked layer filter with multi-scale stencils in a D3000/500–D2000/300–D2000/100 μm configuration achieved a reasonable filter efficiency of 57% even for ultra-fine dust (PM1.0). Figure 4b demonstrates a similar trend for PM2.5. Using a mono-layer stencil as a filter is inadequate, as evidenced by the low filter efficiency of about 30%. However, using a three-stacked layer filter with single-scale stencils improved the filter efficiency of 55% for PM2.5, while a three-stacked layer filter with multi-scale stencils exhibited 75% filter efficiency. Last, the filter efficiency for PM5.0 using the stacked stencil filter with single-scale and multi-scale showed about 90%. Whereas, the mono-layer stencil filter exhibited about 65% for PM5.0, which is still insufficient for the filtering. It is confirmed that the stacking of the stencils acts as an acceptable filter for PMs. Here, the filter efficiency of the three-stacked layer with multi-scale stencils was higher than that with single-scale stencils. This difference in filter efficiency is attributed to the distinction of open ratio, which is the apertured area divided by the overall area, of the two types of stencils. Specifically, the open ratio of multi-scale stencils is 0.04, which is the square of the open ratio of single-scale stencils of 0.2. The fivefold decreased open ratio of the multi-scale stencils leads to five times increase in the inflow face velocity of the particles through the single-hole of multi-scale stencils at the same face velocity compared to the single-scale stencils, as expressed by Equation (2).

$$V_{\text{hole velocity}} = \frac{V_{\text{face velocity}}}{\text{Open ratio}} \quad (2)$$

The aforementioned characteristic of multi-scale stencils promotes efficient particle capture through the impaction to the next layer. In addition, since the multi-scale stencil consists of a layer with large-sized apertures and a layer with small-sized apertures, wall structures are formed around small-sized apertures where the particles pass through. This design would help to stabilize the captured particles and prevent them from bouncing off during the filtering test. Figure S4, Supporting Information, shows a qualitative comparison of filter performance using the OM image. Figure S4a–c, Supporting Information, indicates that

Table 1. The measured pressure drops depending on the configuration of PUA stencil filters.

The composition of assembly PUA polymeric stencils	Pressure Drop [Pa]
D500	0
D300	0
D100	4
D500–D300–D100	5
D3000500–D2000300–D2000100	42

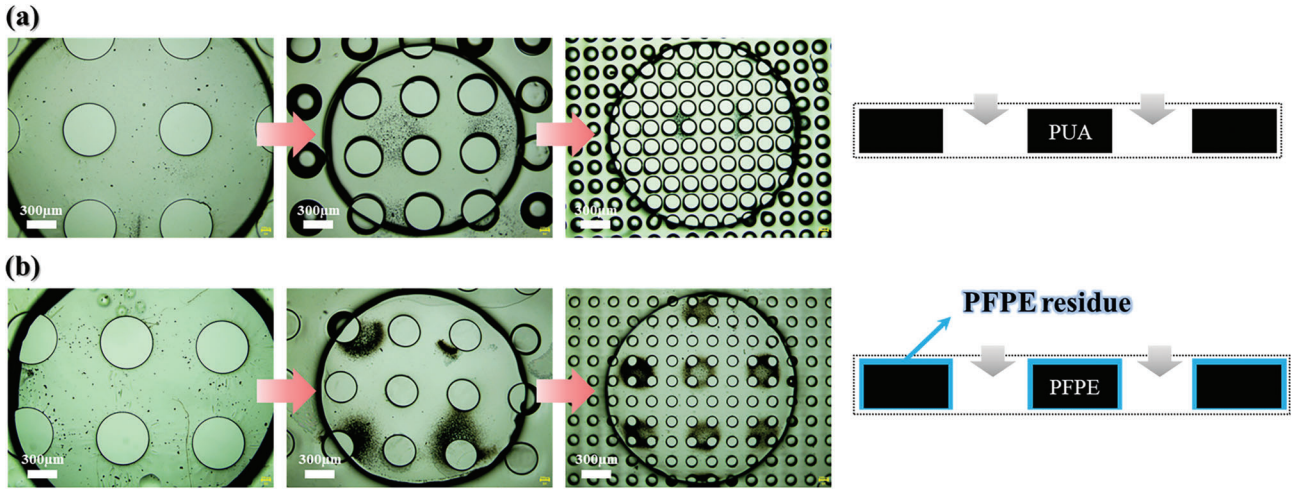

Figure 5. The OM images of the captured particle on the surface of the stencils with a variation of material of the stencil. a) PUA based stencils and b) PFPE based stencils.

confirming particles captured on the surface of mono-layer filters with single-scale stencils is difficult due to their low filter efficiency. In contrast, particles captured by the three-stacked layer filter are more evident. Notably, the three-stacked layer filter with multi-scale stencils (Figure S4d, Supporting Information), which exhibited high filter efficiency, captured a greater amount of particles than the three-stacked layer filter with single-scale stencils (Figure S4e, Supporting Information).

To verify the applicability of the developed stencil filters to PM filter, it is confirmed that the QFs of stencil filters are comparable to the QF standard of commercial fabric filters of 0.02 to 0.04 reported in previous studies.[14,27–29] Not only the three-stacked layer filter with single-scale stencils achieved a QF range of 0.12 to 0.38 at a pressure drop of 5 Pa, which outperformed the QFs of the commercial ones, but also the three-stacked layer filter with multi-scale stencils attained a QF range of 0.02 to 0.06 at a pressure drop of 42 Pa, which is higher than that of the commercial ones.

2.2. The PFPE Polymeric Stencils for Enhanced Filter Efficiency

To further enhance the filtration efficiency, the polymeric multi-scale stencils using perfluoropolyether (PFPE) resin were fabricated. It was reported that the viscoelastic PFPE residue remained after the UV curing process.[30–33] The viscoelastic PFPE residue remaining on the surface of the stencil can improve the filter efficiency by promoting adhesion force between particles and the surface and preventing particle bounce-off. As illustrated in **Figure 5**, it is confirmed that a greater amount of particles was captured to the PFPE stencil surface compared to the PUA stencils, in the same face velocity, spacing between polymeric stencils, and stacking configuration.

Figure 6 indicates that the filter performance, as measured and calculated, is dependent on the material of the polymeric stencils. The three-stacked layer filter with multi-scale PFPE stencils exhibited a higher filter efficiency of 68% compared to the three-stacked layer filter with single-scale PUA stencils (45% filter efficiency) and the three-stacked layer filter with multi-scale PUA stencils (57% filter efficiency) for PM1.0 as shown in Figure 6a. Moreover, the results in Figure 6b indicates that the three-stacked layer filter with multi-scale PFPE stencils obtained better filter efficiency of 85% compared to the three-stacked layer filter with single-scale PUA stencils (55% filter efficiency) and the three-stacked layer filter with multi-scale PUA stencils (75% filter efficiency). Finally, in the case of PM5.0 (Figure 6c), the three-stacked layer filter with multi-scale PFPE stencils exhibits an enhanced

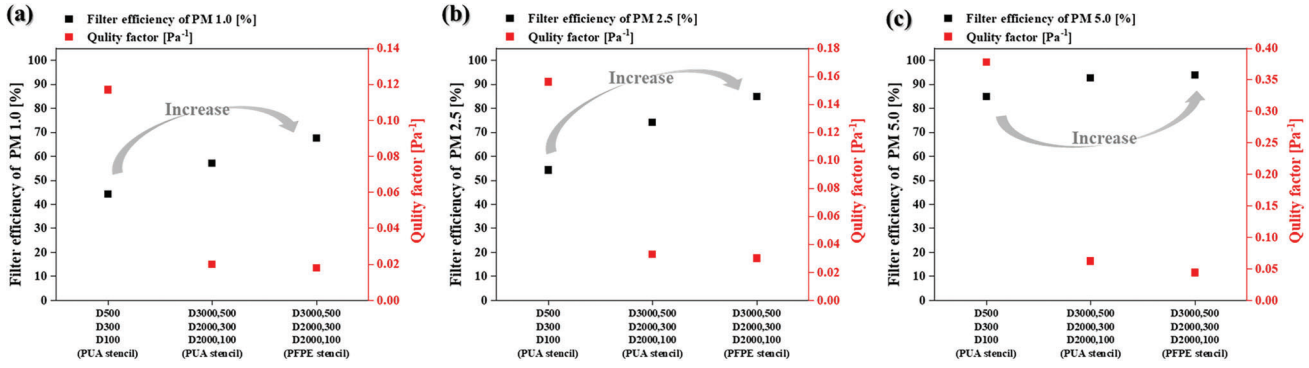

Figure 6. a–c) A plot of filter efficiency and quality factor (QF) of stencil filters depending on the material of stencils for PM1.0 (a), PM2.5 (b), and PM5.0 (c).

Table 2. The measured pressure drops of PUA or PFPE stencil filters.

Material	The composition of assembly polymeric stencils	Pressure Drop [Pa]
PUA	D500–D300–D100	5
PUA	D3000500–D2000300–D2000100	42
PFPE	D3000500–D2000300–D2000100	64

filter efficiency of 94% compared to the three-stacked layer filter with single-scale PUA stencils (85% filter efficiency), while the three-stacked layer filter with multi-scale PUA stencils (93% filter efficiency) showed similar filter efficiency. Based on the results, it implies that the viscoelastic PFPE residue remaining on the surface effectively improves the filter efficiency by enhancing the adhesion force and suppressing the rebound of the impacted particles.

Table 2 shows that the three-stacked layer filter with multi-scale PFPE stencils achieved an improvement in filtration efficiency while slightly increasing a pressure drop (64 Pa) compared to the pressure drop of PUA stencil filters (42 Pa). When comparing the three-stacked layer filter with multi-scale PFPE stencils to the three-stacked layer filter with multi-scale PUA stencils, the QF value slightly decreased while the filter efficiency increased. This suggests that pressure drop is a more influential factor than filter efficiency in determining the QF value. Although the QF value of PFPE-based stencil filters marginally reduced, the values are still acceptable since the QF values range from 0.02 to 0.05, which is analogous to the QF value of the commercialized filter.

2.3. The Mechanism of Impaction-Based Polymeric Stencil Filters

To address the filtration mechanism of the polymeric stencil filters developed in this study, we utilized the COMSOL simulation program to conduct finite element analysis of inflowing particles, as presented in **Figure 7**. The simulation results indicate that the open area and hole geometry of the stencil determine the velocity of incoming particles. The incoming particles have a maximum velocity at the center of the stencil holes, while the minimum velocity is at the blocked area between the holes. As a result, the particles heading straight into the blocked area between holes are abruptly deflected toward the holes. Even during the flow deflection toward the holes, the accelerated particles that stray from the streamline hit the blocked area based on inertia. From the result, the mono-layer stencil cannot be used as a filter due to the absence of the impaction spot for the accelerated particles through the mono-layer stencil hole. To function as a filter, the stencil should be stacked in a multi-layer. For the stacked stencil filters, the accelerated particles are impacted onto the next layer and stacked on the blocked area. This inertia-based impaction is a key mechanism in this particle filtration system. The OM image of the polymeric stencil filters presented in Figure S4, Supporting Information, confirms that particles adhere to only the blocked area between the holes, just like the results of the simulation study.

2.4. The Advantages of Impaction-Based Polymeric Stencil Filters

To compare the relative filtering capacity of commercial fabric filters (HEPA filter; H13) and impaction-based stencil filters (three-stacked layer filters with multi-scale stencil made with PUA and PFPE), the pressure drop for the filters during the particle capturing process was monitored, with a fixed face velocity of 10 cm s^{-1}. The result depicted in **Figure 8a** confirms that the pressure drop of the HEPA filter increased rapidly over operation time due to the particle trapping and clogging of pores inside the HEPA filter. Figure 8b shows the particles are densely accumulated and the pores inside the HEPA filter were significantly clogged. However, the pressure drops of the three-stacked layer stencil filters were stably maintained even when particles were captured inside the filter as shown in Figure 8c. This result highlights the superior filter capacity of stencil filters compared to commercial fabric-based filters. The stencil filters have enough storage space between the stencil layers for particle capturing and stacking.

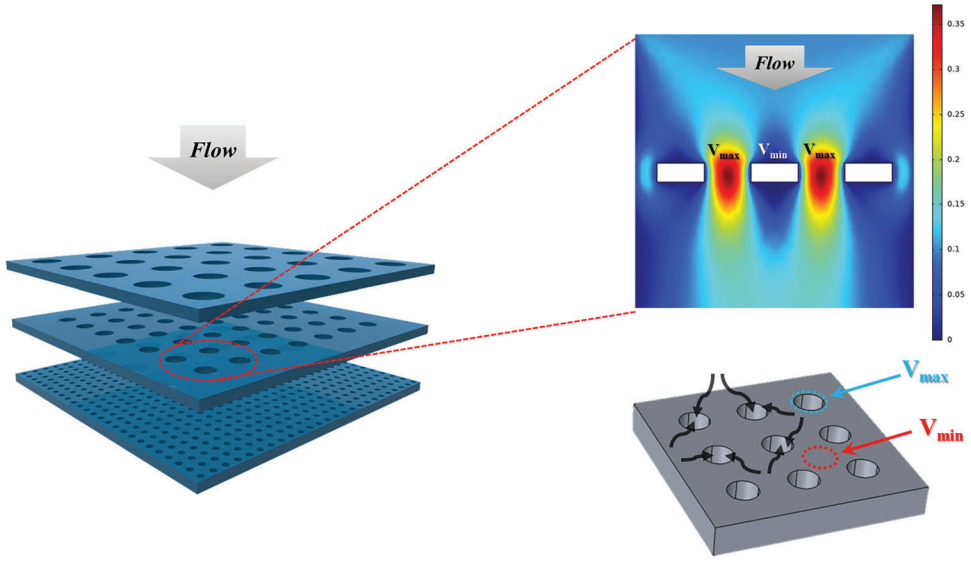

Figure 7. Simulation study of flow velocity through the stencil structure.

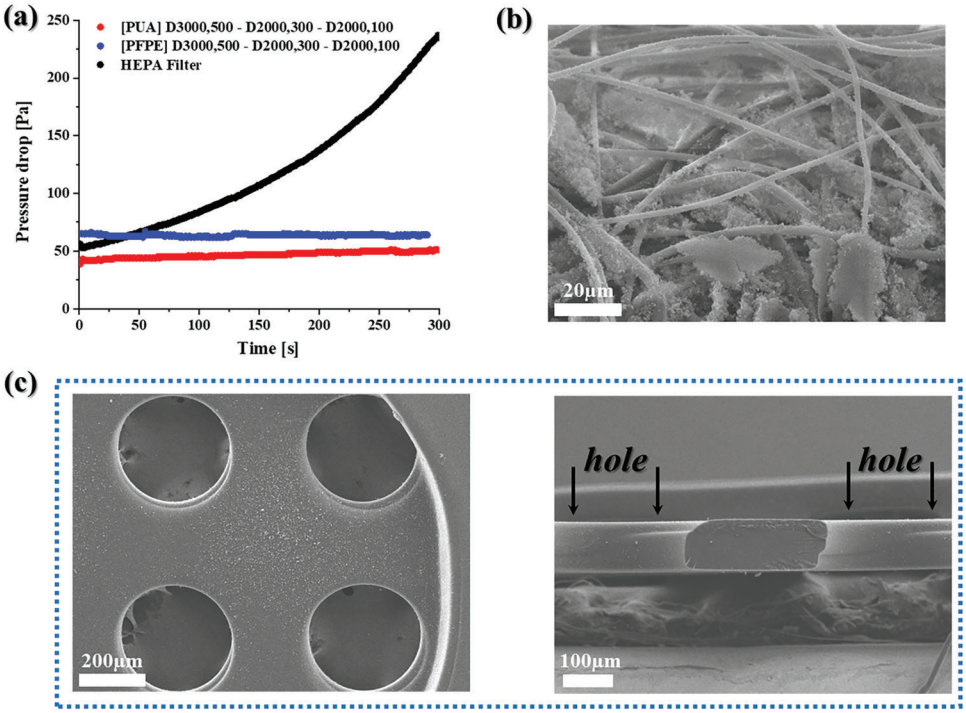

Figure 8. Comparison of filter capacities for commercial HEPA filters and impaction-based stencil filters. a) A plot of the measured pressure drop over filtration time for HEPA filters and stencil filters. b) Cross-sectional SEM image of a HEPA filter after a filtration test. c) Top view and cross-sectional SEM images of a stencil filter after a filtration test.

And as stencil filters capture the particles through the impaction to the blocked area, it prevents clogging of the holes enabling the pressure drop to be stable. When it comes to clogging issue, we further emphasized the critical importance of adjusting the aperture size in accordance with the size of PM for continuous filtration with high filter capacity. The impaction-based filtration mechanism differs from hole-sieving filtration that particles, accelerated as they pass through the nozzle, are filtered as they impact the obstructed flat space in the subsequent layer. As such, when the aperture size of the isoporous membrane closely matches the size of the PM to be filtered, the apertures can become clogged, leading to a rapid increase in pressure drop, which significantly diminishes filter capacity. To validate this concern, we fabricated polymeric stencil filters featuring 5 μm aperture size and conducted a filtering test. Figure S5, Supporting Information, provides a comparative analysis of filter efficiency and filter capacity, utilizing a stencil with 5μm-aperture size and a stencil with an minimum 100 μm-aperture size. In the case of the D50, 5 μm multi-scale stencil filter, it exhibited a high filter efficiency of 73.02% for PM2.5 and 97.73% for PM5.0. However, it experienced issues with filter capacity due to aperture clogging resulting from particle accumulation during operation, leading to a rapid increase in pressure drop. In contrast, the three-stacked layer filter with an minimum 100 μm-aperture size maintained comparable filter efficiency, with the pressure drop remaining constant over the operation duration without aperture clogging, affirming its high filter capacity. With the increased energy consumption associated with low filter capacity and rising pressure drop, it has become evident that selecting the aperture size in accordance with the particle generation environment is paramount to ensure both adequate filter efficiency and filter capacity.

Furthermore, we have fabricated the multi-scale stencil with D50, 0.8 (800 nm) aperture and conducted filtering test with it. As shown in Figure S6, Supporting Information, ultra-thin thinness of 800 nm apertured layer can lead to tearing during the stencil manufacturing process and damage due to the pressure exerted by the flow during operation. Such stencil damage can compromise the proper functionality of the filter. The result indicates the importance of considering not only the pore size but also the pore depth, which determines the thickness of the stencil, particularly in relation to the filtering conditions including flow velocity through the apertured layer. This careful consideration ensures the mechanical robustness necessary for reliable filter performance.

Reducing pressure drop and maintaining the pressure drop stably during the filtering process is crucial in the aspect of energy efficiency and user comfort. In the application of air filters for capturing fine dust, to achieve effective filtering, more electrical energy from compressors and pumps is required as the pressure drop increase. When the pressure drops excessively increases, it leads to the failure of the filtering system. In addition, when the filter is applied to a facial mask, a higher-pressure drop can cause difficulty in breathing and discomfort during daily activities. To ensure user comfort and health, it is essential to reduce pressure drop and maintain the pressure drop stably with sufficient filter efficiency.

The polymeric stencil filters offer additional benefits including reusability and a simple cleaning process. As mentioned above, the particles in the commercial fabric filters, which are composed

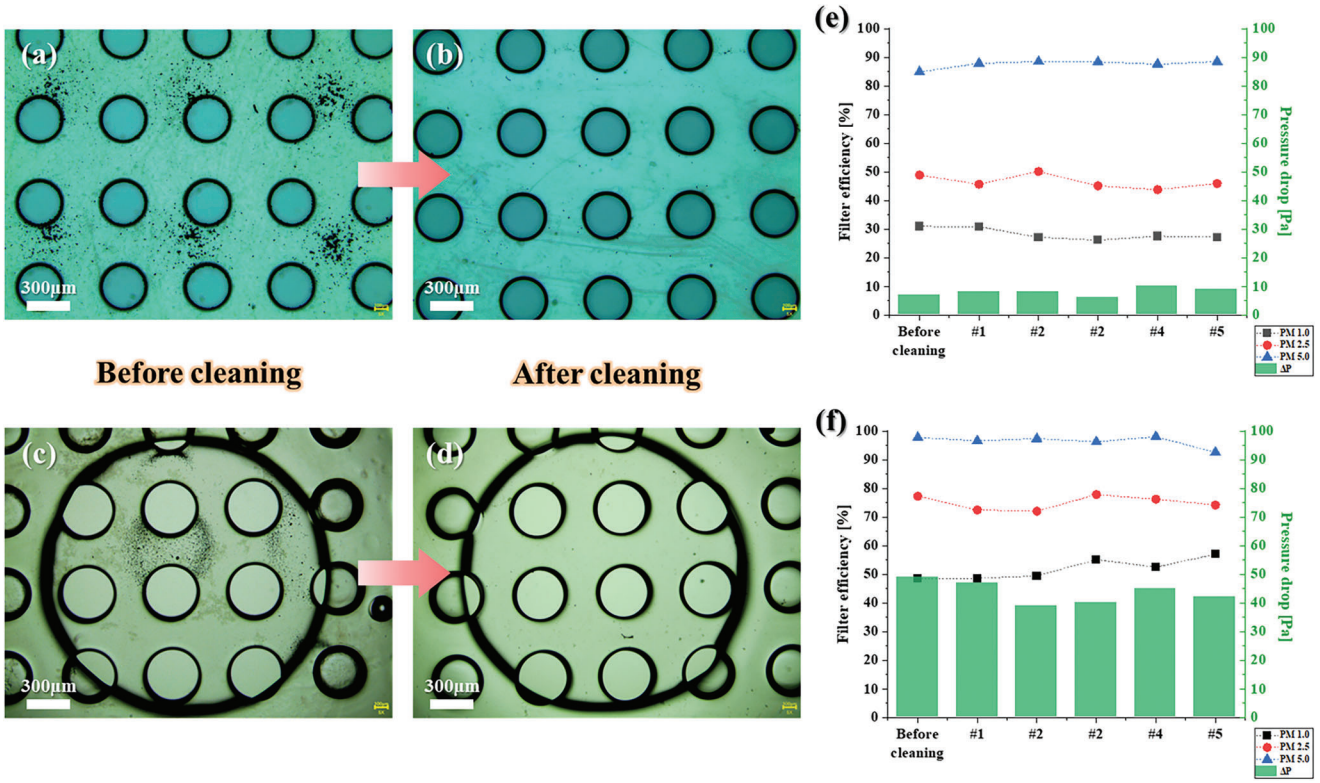

Figure 9. Demonstration of reusability of stencil filters. a–d) OM images of polymeric stencil filters a,c) before cleaning and b,d) after cleaning using DI water and ethanol. e,f) Measured filter efficiency and pressure drop depending on the number of cleanings with e) the three-stacked layer filter with single-scale, and f) the three-stacked layer filter with multi-scale.

of stacked layers, are trapped deeply and are hardly to be removed by cleaning. And the previous research presents that when washing melt-blown nonwoven fabric and cloth masks with 75% ethanol, the pore sizes of these masks increased, resulting in reduced filtration performance after the washing and drying cycle, indicating that the masks cannot be reused.[34] In contrast, the developed stencil filters can be easily cleaned and reused by removing the captured particles on the stencil surface with DI water or ethanol washing for a few seconds. As shown in **Figure 9**a–d of OM images with the stencil surface before and after cleaning, the adsorbed particles were removed by cleaning and the surface of the stencils after cleaning appeared immaculate. To further demonstrate the reusability of the polymeric stencil as a filter, the filtration tests were repeated five more times after cleaning at every cycle with both the three-stacked layer filter with a single-scale and multi-scale. Figure 9e,f shows that the filter efficiency and pressure drop remained consistent even after every cleaning process, maintaining the analogous performance as the initial state. And to verify whether sterilization by ethanol washing is effective, additional experiments were performed. The fungi originating from the hand and saliva were cultured on the stencil placed on agar gels in the high RH and 39 °C conditions for 7 days. Subsequently, the stencils were washed with 70% ethanol. Figure S7, Supporting Information, provides visual evidence of fungal growth on the stencil surface before washing and successful sterilization after washing. Notably, after washing with 70% ethanol, we confirmed the disappearance of the fungi covering the surface. There was no alteration in the shape and size of the stencil filter before and after washing. This observation indicates the reusability of the stencil filter after effective sterilization.

To demonstrate the availability of the polymeric stencil filter even in high and low-temperature conditions, the stability of polymeric stencils under varied temperature conditions was investigated. To assess the deformation of polymeric stencils under different temperature conditions, the polymeric stencil was exposed to a temperature range from −196 to 450 °C for 30 min at each fixed temperature. **Figure 10** presents the OM images of the single-layer polymeric stencil after exposing to 25, 350, 400, and 450 °C. The temperature was raised by 50 °C every 30 min until reaching 450 °C. After the thermal treatment, the shrinkage ratio in length was 3% at 350 and 400 °C, and 7% at 450 °C compared to the initial state. It is noted that the shape and morphology of the apertures in the stencil were almost unchanged even at the high temperature, implying excellent thermal stability. In the case of the multi-scale polymeric stencil, a comparable shrinkage in length, and undeformed apertures were observed when exposed to high temperatures like the single-scale stencil (Figure S8, Supporting Information). However, while the polymeric stencil was flexible after the thermal treatment up to 400 °C, it became brittle after the thermal treatment at 450 °C, which may come from thermal decomposition and oxidation. This suggests that polymeric stencil filters can be used at temperature conditions below 400 °C. Notably, PM emissions from industrial field activities, coal combustion, and vehicle combustion,

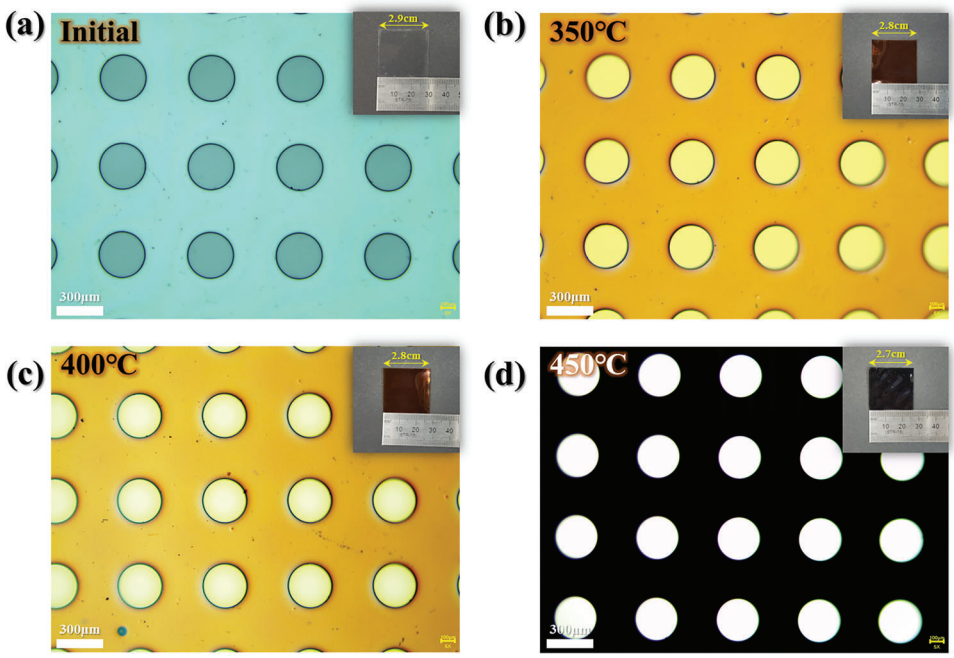

Figure 10. Demonstration of thermal stability of polymeric stencil filter with single-scale. OM image of the stencil filter a) at initial state (25 °C), b) after exposure to 350 °C, c) after exposure to 400 °C, and d) after exposure to 450 °C.

the primary contributors to PM2.5 emissions, typically occur at high temperatures ranging from 50 to 300 °C.[35,36] Hence, the polymeric stencil filters with high thermal stability can serve as a valuable component for capturing fine dust stably and effectively even in high-temperature environments. Additionally, it is observed that the polymeric stencils are stable even under extremely low temperatures. Figure S9, Supporting Information, illustrates the results of morphology change for single-scale and multi-scale polymeric stencils after being immersed in liquid nitrogen at −196 °C for 30 min, demonstrating that no shrinkage occurred even in cryogenic conditions. Consequently, the polymeric stencil filters can be widely and stably applied across a broad range of temperature conditions, spanning from −197 to 400 °C.

In addition, to clearly demonstrate the transparency of the stencil filters, the optical transmittance of the stencil filters and commercial filters in visible wavelength ranging from 400 to 800 nm was measured by UV–vis spectrophotometer, as shown in **Figure 11**. The transmittance values for the fabric filters were measured to be 27% for a HEPA filter and 15% for a KF94 health

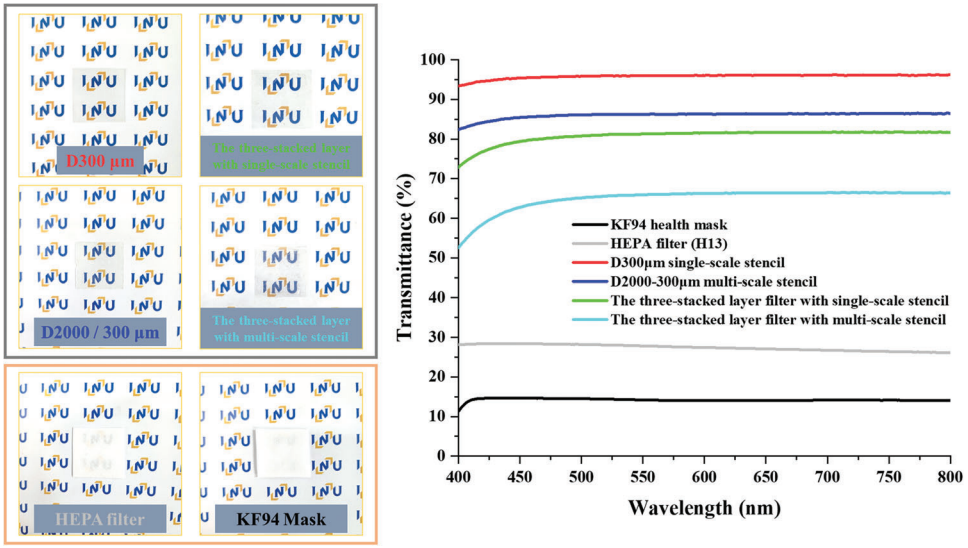

Figure 11. Measured optical transmittance of the stencil filters and commercial fabric filters in visible wavelength.

mask filter. In contrast, the polymeric stencil filter exhibited significantly higher transmittance when compared to these commercial filters. Specifically, the transmittance for the polymeric stencil filters were as follows: 96% for a single-scale stencil, 86% for a multi-scale stencil, 82% for a three-stacked layer filter with a single-scale stencil, and 66% for a three-stacked layer filter with a multi-scale stencil. To visually confirm this, each filter was placed on a mark sheet, and a camera image was taken. As a result, the mark under the commercial filter was barely visible, but it was confirmed that the mark was clearly visible even when a transparent stencil filter was layered.

3. Conclusion

In this study, we developed a reusable and transparent impaction-based filter using micro-apertured polymeric stencils for capturing PMs. The filtering tests with the polymeric filters were conducted with a variation of operating conditions including the inlet face-velocity of particles, the spacing between polymeric stencils, and the stacking configuration using single-scale and multi-scale polymeric stencils, respectively. Following obtained proper operating conditions, the inlet face velocity is 10 cm s^{-1}, the spacing between stacked polymeric stencils is 0.2 mm for top two layers and 0.1 mm for bottom two layers, and the polymeric stencil filters with the smaller holes were placed toward the bottom. As a result, the highest filter efficiency was obtained under a three-stacked layer filter with multi-scale PUA stencils as 57% (PM1.0), 75% (PM2.5), and 93% (PM5.0) with a low-pressure drop of 42 Pa. The three-stacked layer filter with multi-scale PFPE stencils showed further enhanced performance as 68% (PM1.0), 85% (PM2.5), and 94% (PM5.0) with a low-pressure drop of 64 Pa by promoting adhesion force between particles and the surface and preventing particle bounce-off utilizing the viscoelastic PFPE residue on the surface of stencils. In terms of QFs, the three-stacked layer filter with multi-scale stencils has a QFs range of 0.02 to 0.06, which is higher than that of the commercial filters. It indicates the impaction-based stencil filters are highly applicable for effective capturing by facilitating the effect of the impaction mechanism which is also confirmed by COMSOL simulation study reflecting the actual filtration process. Consequently, the developed and optimized polymeric stencil filters exhibited sufficient filter efficiency, superior filter capacity, and lower pressure drop rate. In addition, it is proved that the polymeric stencil filters can be reused multiple times by simply washing process using DI water or ethanol while maintaining filter performance even after every washing cycle. And the polymeric stencil showed excellent stability without morphological change of the apertures in the stencil even when exposed to high temperatures at 450 °C and cryogenic temperatures at −197 °C. These findings highlight the promising potential of impaction-based polymeric stencil filters for effective capturing PM in a wide range of applications, including industrial, indoor, and vehicle components. Moreover, this flexible and transparent polymeric stencil filters can be applied to transparent facial health mask, as illustrated in Figure S10, Supporting Information. The advances would offer enhanced breathability and visibility while providing effective filtration capabilities.

4. Experimental Section

UV Curable Materials: Commercially available UV-curable PUA resin (MINS-311RM, Changsung Sheet) and PFPE resin (MD 700, Solvay) were used in the experiment. The PFPE prepolymer resin was prepared by mixing MD 700 and 2-hydroxy-2-methylpropiophenone as a photo-initiator (3 wt%).

Preparation of the Micro-Dot Patterned PDMS Mold: To prepare the patterned PDMS molds, the patterned silicon master molds were fabricated using photolithography and reactive ion etching to create micro-dot apertures. The surface of the silicon master mold was treated with C_4F_8 gas to facilitate the separation of the patterned PDMS polymer in detach process. Next, the mixture of PDMS base (Sylgard 184 PDMS elastomer, Dupont) and curing agent with a weight ratio of 10:1 was poured onto the patterned silicon master mold and cured for 2 h at 70 °C. Finally, the cured PDMS molds were carefully detached from the silicon master mold.[37,38]

Fabrication of the Polymeric Stencils with Single/Multi-Scale Apertures: The fabrication process of a single-scale and multi-scale polymeric stencil with a stable upright micro aperture is illustrated in **Figure 12**. To manufacture the single-scale polymeric stencil, as depicted in Figure 12a, PUA or PFPE prepolymer resin is dispensed onto a micro-pillar patterned PDMS mold, and a flat PDMS mold is placed on the prepolymer resin. The prepared stacked assembly (patterned PDMS mold/UV curable prepolymer resin/flat PDMS mold) was cured under UV light (F8T5BL, SANKYO DENKI, $\lambda \approx 352$ nm) of 20 W cm^{-2} for ≈1 min. After turning off the UV exposure and detaching the flat PDMS mold from the stacked layer, the cured PUA or PFPE stencil was carefully detached from the micro-pillar patterned PDMS. Similarly, to manufacture the multi-scale stencil, as shown in Figure 12b, a micro-pillar patterned PDMS mold with different dimensions was used instead of a flat PDMS mold. The prepared stacked assembly (patterned PDMS mold/UV curable prepolymer resin/patterned PDMS mold) was cured for ≈2 min using the same process. In the process depicted in Figure 12, the gas permeability of PDMS allows oxygen gas to permeate into the skin surface of the prepolymer layers, creating an oxygen-infiltrated layer, as previously studied. The presence of oxygen gas in this layer causes a delay in the UV curing process, known as the oxygen-scavenging effect. When the surfaces of both PDMS molds get close to coming into contact, the overlapped OILs further delay UV curing, ultimately leading to the formation of apertures in the polymeric stencil structures.[37] Finally, the fabricated PUA stencils were exposed to UV light without any external load in the UV exposure equipment for more than 6 h to perfectly cure the uncured slightly PUA prepolymer residue on its surface.

Particulate Matter Filtration System Set-Up: The experimental setup used to measure the filtration performance of polymeric stencil filters is shown in **Figure 13**, and the camera image of the experimental setup is presented in Figure S11, Supporting Information. The PM was generated using an aerosol generator (Aerosol Generator2, Sant) with Arizona dust (A2 fine test dust, POWDER TECHNOLOGY INC.). As indicated in Figure 13, the air compressor was turned on, and the compressed air was cleaned by passing through 5 µm, and adsorbent filters before inflowing into the atomizer. Inside the atomizer, a diluted PM solution was aerosolized. The generated aerosol particles passed through a diffusion dryer to remove humidity before flowing into the installed polymeric stencil filter, which was sandwiched between the acrylic holder. To measure and compare the filter performance, a particle counter (LP301, LP AIR) was installed at the front and rear end of the fixed assembly polymeric stencil filters. The pressure drop through the differential pressure gauge (Testo 510, Testo) was also measured during the operation of the filtration system to monitor the filter's performance. Additionally, the flow velocity of PM inflowing through the flow meter (RMA-14-SSV, RMA-22-SSV, Dwyer) was adjusted and determined to ensure the accurate measurement of PM filtration efficiency.

Physical Analysis: SEM images were obtained using field emission SEM (FE-SEM, JSM-7800F, JEOL) with 15.0 kV acceleration voltage to confirm the stable upright holes of polymeric stencils and the captured particles inside of the filter. Optical microscope (OM) images were obtained by optical microscopy (BX53M, Olympus) to observe the particles captured

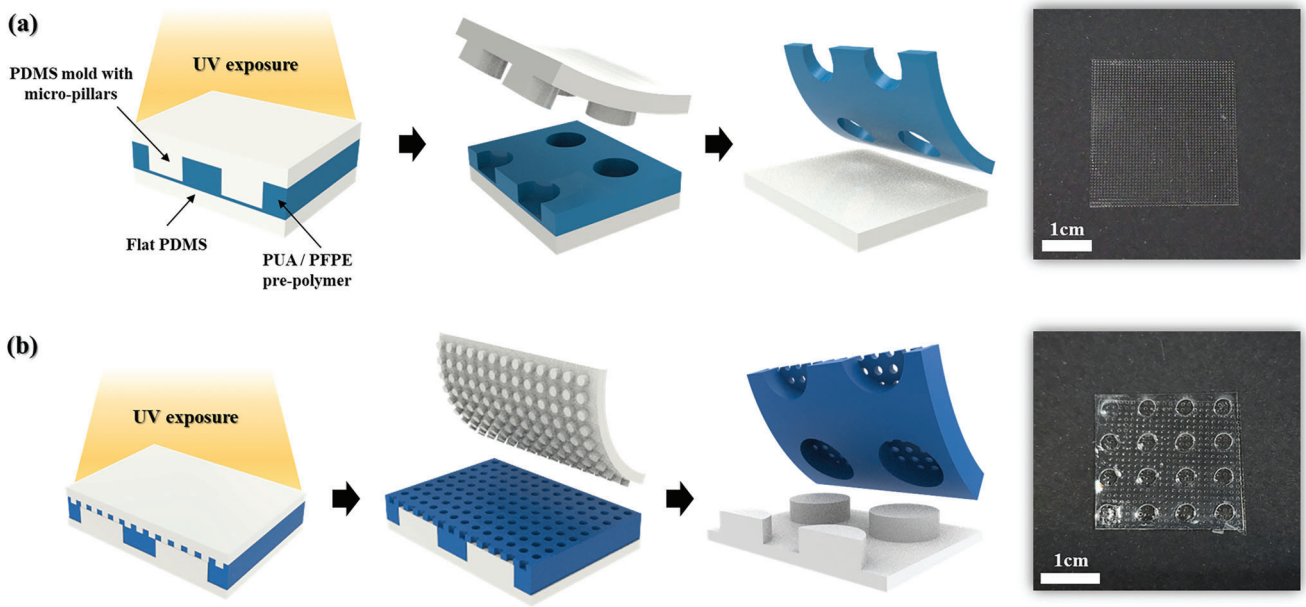

Figure 12. Schematic of the fabrication process of polymeric stencils with stable upright micro apertures using PUA/PFPE prepolymer. a) The process of single-scale polymeric stencils. b) The process of multi-scale polymeric stencils.

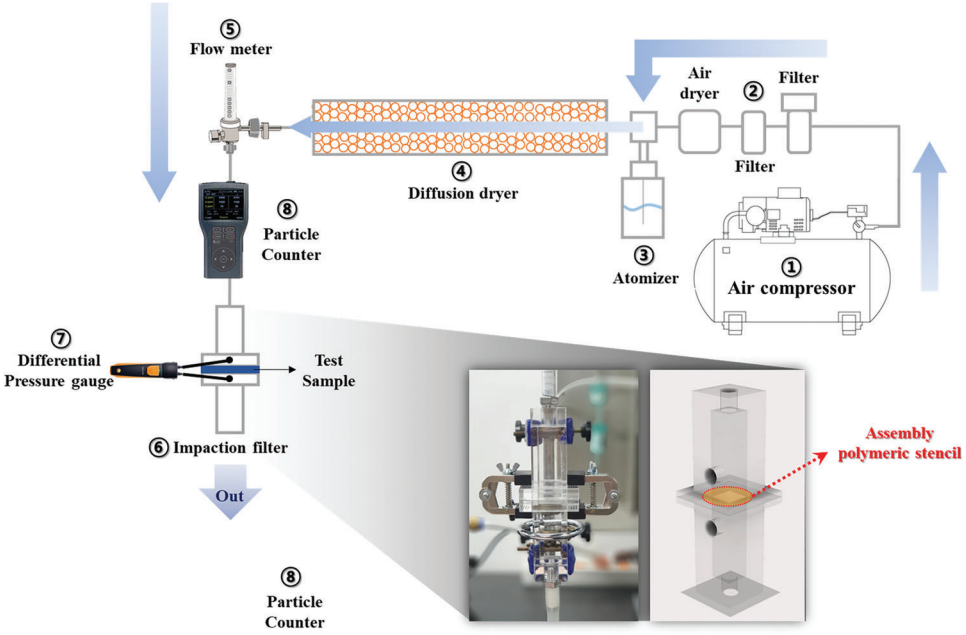

Figure 13. Schematic illustration of the experimental setup to measure filter performance.

on the surface of polymeric stencils. The optical transmittance of the stencil filters and commercial filters in visible wavelength ranging from 400 to 800 nm was measured by UV–vis spectrophotometer (UV-2600, SHIMADZU).

Supporting Information

Supporting Information is available from the Wiley Online Library or from the author.

Acknowledgements

This work was supported by the National Research Foundation (NRF) of Korea (NRF-2019R1C1C1006392 and 2021R1C1C1010589).

Conflict of Interest

The authors declare no conflict of interest.

Data Availability Statement

The data that support the findings of this study are available from the corresponding author upon reasonable request.

Keywords

impaction based filter, particulate matter, polymer membrane, reusable, transparent

Received: August 11, 2023
Revised: September 19, 2023
Published online: November 22, 2023

[1] H. R. Anderson, *Lancet Respir. Med.* **2017**, *5*, 916.
[2] W. Chen, Q. Ou, X. Liu, M. Maricq, Z. Pan, D. Kittelson, D. Y. H. Pui, *Sep. Purif. Technol.* **2023**, *315*, 123658.
[3] W.-Y. Jiang, R. Wang, X.-F. Pan, Y.-Z. Shen, T.-X. Chen, Y.-H. Yang, J.-C. Shao, L. Zhu, B.-H. Han, J. Yang, H. Zhao, *J. Thorac. Dis.* **2016**, *8*, 2610.
[4] M. Li, Y. Feng, K. Wang, W. F. Yong, L. Yu, T.-S. Chung, *Environ. Sci. Technol.* **2017**, *51*, 10041.
[5] C.-S. Liang, F.-K. Duan, K.-B. He, Y.-L. Ma, *Environ. Int.* **2016**, *86*, 150.
[6] R. M. Harrison, *Sci. Total Environ.* **2004**, *334*, 3.
[7] J. Yin, A. G. Allen, R. M. Harrison, S. G. Jennings, E. Wright, M. Fitzpatrick, T. Healy, E. Barry, D. Ceburnis, D. Mccusker, *Atmos. Res.* **2005**, *78*, 149.
[8] C. Ehrlich, G. Noll, W. Kalkoff, G. Baumbach, A. Dreiseidler, *Atmos. Environ.* **2007**, *41*, 6236.
[9] F. Costabile, M. Gualtieri, C. Ancona, S. Canepari, S. Decesari, *Atmosphere* **2020**, *11*, 414.
[10] J. P. Dudeja, *Int. J. Acad. Res. Dev.* **2018**, *3*, 576.
[11] Z. Shao, H. Chen, Q. Wang, G. Kang, X. Wang, W. Li, Y. Liu, G. Zheng, *Sep. Purif. Technol.* **2022**, *302*, 122175.
[12] S.-J. Choi, K. Kim, H. Kim, J. Yoon, M. Lee, K.-S. Choi, U.-D. Sung, W.-T. Park, J. Lee, J. Jeon, J. Im, K.-K. Kim, S. Cho, *Appl. Sci.* **2019**, *9*, 235.
[13] S. Wang, X. Zhao, X. Yin, J. Yu, B. Ding, *ACS Appl. Mater. Interfaces* **2016**, *8*, 23985.
[14] Y. H. Choi, J. Lee, D.-Y. Khang, *J. Membr. Sci.* **2020**, *612*, 118474.
[15] H. Ma, B. S. Hsiao, in *Current Trends and Future Developments on (Bio-) Membranes* (Ed: A. Basile, E. Curcio, Inamuddin), Elsevier, New York **2019**, pp. 81–104.
[16] R. Gopal, S. Kaur, Z. Ma, C. Chan, S. Ramakrishna, T. Matsuura, *J. Membr. Sci.* **2006**, *281*, 581.
[17] Y. Liu, H. Shao, H. Wang, Z. Ji, R. Bai, F. Chen, B. Li, C. Chang, T. Lin, *Adv. Mater. Interfaces* **2022**, *9*, 2101848.
[18] D. Park, M. Kim, S. Lee, I.-J. Yoon, K. Lee, M. H. Lee, J. Nah, *Adv. Mater. Interfaces* **2019**, *6*, 1801832.
[19] J. Xue, T. Wu, Y. Dai, Y. Xia, *Chem. Rev.* **2019**, *119*, 5298.
[20] W. J. Li, C. T. Laurencin, E. J. Caterson, R. S. Tuan, F. K. Ko, *J. Biomed. Mater. Res.* **2002**, *60*, 613.
[21] R. Chen, H. Zhang, M. Wang, X. Zhang, Z. Gan, *ACS Appl. Nano Mater.* **2020**, *4*, 182.
[22] R. Barhate, S. Ramakrishna, *J. Membr. Sci.* **2007**, *296*, 1.
[23] Y. Yao, S. Liu, T. You, Z. Zhou, X. Zhang, M. Tang, Z. Sun, J. Wang, J. Hu, *Sep. Purif. Technol.* **2022**, *295*, 121263.
[24] M. Kim, J. Lee, J. Kim, S. Jang, S. M. Kim, *Polymers* **2021**, *13*, 4361.
[25] T. Joo, M. Takeuchi, F. Liu, M. P. Rivera, J. Barr, E. S. Blum, E. Parker, J. H. Tipton, J. Varnedoe, B. Dutta, R. P. Lively, N. L. Ng, *Aerosol Sci. Technol.* **2021**, *55*, 930.
[26] D. Shou, J. Fan, L. Ye, H. Zhang, X. Qian, Z. Zhang, *J. Nanomater.* **2016**, *16*, 351.
[27] S. Sankhyan, K. N. Heinselman, P. N. Ciesielski, T. Barnes, M. E. Himmel, H. Teed, S. Patel, M. E. Vance, *Aerosol Air Qual. Res.* **2021**, *21*, 210117.
[28] C. Liu, P.-C. Hsu, H.-W. Lee, M. Ye, G. Zheng, N. Liu, W. Li, Y. Cui, *Nat. Commun.* **2015**, *6*, 6205.
[29] L.-Y. Wang, W. F. Yong, L. E. Yu, T.-S. Chung, *J. Membr. Sci.* **2017**, *535*, 342.
[30] C. Ursino, E. Di Nicolò, B. Gabriele, A. Criscuoli, A. Figoli, *J. Membr. Sci.* **2019**, *581*, 58.
[31] H.-W. Park, H.-S. Seo, K. Kwon, S. Shin, *RSC Adv.* **2023**, *13*, 11874.
[32] C.-M. Ryu, B.-L. Pang, J.-H. Han, H.-I. Kim, *J. Photopolym. Sci. Technol.* **2012**, *25*, 705.
[33] H. Cho, J. Kim, H. Park, J. W. Bang, M. S. Hyun, Y. Bae, L. Ha, D. Y. Kim, S. M. Kang, T. J. Park, S. Seo, M. Choi, K.-Y. Suh, *Nat. Commun.* **2014**, *5*, 3137.
[34] X. Shan, H. Zhang, C. Liu, L. Yu, Y. Di, X. Zhang, L. Dong, Z. Gan, *ACS Appl. Mater. Interfaces* **2020**, *12*, 56579.
[35] X. Yang, Y. Pu, S. Li, X. Liu, Z. Wang, D. Yuan, X. Ning, *ACS Appl. Mater. Interfaces* **2019**, *11*, 43188.
[36] H. Wang, S. Lin, S. Yang, X. Yang, J. Song, D. Wang, H. Wang, Z. Liu, B. Li, M. Fang, N. Wang, H. Wu, *Small* **2018**, *14*, 1800258.
[37] H. Cho, S. S. Kim, Y. S. Kang, J. Kim, S. Jang, M. Kim, H. Park, J. W. Bang, S. Seo, K.-Y. Suh, Y.-E. Sung, M. Choi, *Nat. Commun.* **2015**, *6*, 8484.
[38] C. Seol, S. Jang, J. Kim, T.-S. Jun, S. M. Kim, *Soft Matter* **2018**, *14*, 9522.

